

# Common complex biochemical processes exhibit simple completion time distributions

Golan Bel,<sup>1,2,\*</sup> Brian Munsky,<sup>1,2,†</sup> and Ilya Nemenman<sup>1,‡</sup>

<sup>1</sup>Center for Nonlinear Studies and Computer, Computational and Statistical Sciences Division,  
Los Alamos National Laboratory, Los Alamos, NM 87545 USA

<sup>2</sup>Contributed Equally

Biochemical processes typically involve huge numbers of individual steps, each with its own dynamical rate constants. For example, kinetic proofreading processes rely upon numerous sequential reactions in order to guarantee the precise construction of specific macromolecules [Hopfield, 1974]. In this work, we study the transient properties of such systems and fully characterize their first passage time (completion) distributions. In particular, we provide explicit expressions for the mean and the variance of the kinetic proofreading completion time. We find that, for a wide range of parameters, as the system size grows, the completion time behavior simplifies: it becomes either deterministic or exponentially distributed, with a very narrow transition between the two regimes. In both regimes, the full system dynamical complexity is trivial compared to its apparent structural complexity. Similar simplicity will arise in the dynamics of other complex biochemical processes. In particular, these findings suggest not only that one may not be able to understand individual elementary reactions from macroscopic observations, but also that such understanding may be unnecessary.

PACS numbers:

## I. INTRODUCTION

Considering the ever increasing quantity of known biochemical reactions, one cannot help but be amazed and daunted by the incredible complexity of the implied cellular networks. For example, just a handful of different proteins can form a combinatorially large number of interacting molecular species, such as in the case of immune signaling [1], where multiple receptor modification sites result in a model with 354 distinct chemical species. One must then ask: When do all details of this seemingly incomprehensible complexity actually matter, and when is there a smaller set of aggregate, coarse-grained dynamical variables, parameters, and reactions that approximate the salient features of the system's dynamics? What determines which features are relevant and which are not? And if the networks have a simple equivalent dynamics, did nature choose to make them so complex in order to fulfill a specific biological function? Or is the unnecessary complexity a "fossil record" of the evolutionary heritage?

In this article, we begin investigation of these questions in the context of certain specific biochemical kinetics networks, namely a reversible linear pathway, a *kinetic proofreading* (KPR) scheme [2], and their combination. These motifs are common in a variety of cellular processes, where assembly of specific biochemical structures requires multiple steps to amplify small differences between very similar bimolecular building blocks. Such motifs are present in DNA synthesis and repair [3, 4], pro-

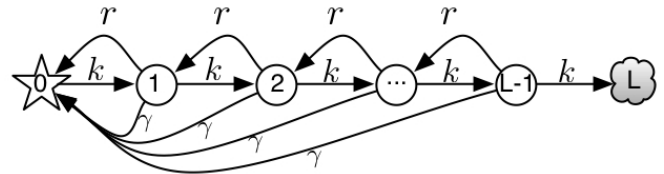


FIG. 1: Schematic description of the model. The process begins at the site  $i = 0$ , represented with a star. At each site, the process may transition one step to the right with the forward rate  $k$ , one step to the left with the backward rate  $r$ , or all the way back to the origin with the return rate  $\gamma$ . The right-most site,  $i = L$  is an absorbing site (cloud) at which the process is completed.

tein translation [2, 5], molecular transport [6], receptor-initiated signaling [7, 8, 9, 10, 11, 12], and other processes. However, in this article, we leave aside the functional behavior of these networks and focus instead on a different question: do these complex kinetic schemes have a simplified, yet accurate description? Since the structural complexity (see Fig. 1) is crucial for the performance a KPR process, this system is well suited for the analysis.

We show analytically and numerically that, over a broad range of parameters, the kinetic schemes exhibit the behavior of either a deterministic process, or a single-step exponential-waiting-time process. We also propose intuitive arguments for the result, which leads us to believe that similar simplifications of complex behavior may be wide-spread, and even universal. However, a detailed analysis of this conjecture is left for a future work.

\*Electronic address: golanbel@lanl.gov

†Electronic address: brian.munsky@gmail.com

‡Electronic address: nemenman@lanl.gov

## A. The Model

For this study we utilize a general KPR (gKPR) model [2], for which many properties can be computed analytically. The model is represented by the Markov chain in Fig. 1. At time  $t = 0$ , the dynamics begins at the point represented by the star ( $i = 0$ ). The process can leave this state at some exponentially distributed waiting time, defined by a *forward rate*  $k$ , and the process can continue in the forward direction with rate  $k$  until it reaches the final absorbing point (cloud) at  $i = L$ . At each interior point,  $i \in \{1, 2, \dots, L-1\}$ , the process can also move one step to the left with a *backward rate*  $r$  or all the way back to the origin with a *return or proofreading rate*  $\gamma$ . The forward and the backward rates emphasize the reversibility of all reactions, and the return rate corresponds to a catastrophic failure, after which the whole process must start anew. For example, in immune signaling,  $\gamma$  would represent the rate of receptor-ligand dissociation, which destroys receptor cross-linking and prevents future forward events for a relatively long period of time [1].

This model is substantially simplified compared to detailed models of real biological processes [1] in that, in nature, all three rates may depend on  $i$ , and the nodes may not form a linear chain. However, in order to better understand these more complicated schemes, it is reasonable to first obtain a detailed understanding of this simplified model.

## B. The Relevant Features

To determine if a kinetic model can be well approximated by a simpler one, we must first decide which of its features must be retained. To illustrate this question, consider the activation of a signaling cascade specified in Fig. 1 by an extracellular ligand. The ligand binding initiates the process, bringing it from state  $i = 0$  to state  $i = 1$ . With the exception of this transition, the extracellular environment does not affect the process. Similarly, the downstream signaling pathways are only affected when the signalign construct attains its fully activated state at  $i = L$ . Thus, as far as the rest of the cell is concerned, only the times of process initiation and completion are controllable, observable or otherwise important. That is, the system can be characterized by the distribution of the *first passage* or the *escape time* between the release at  $i = 0$  at  $t = 0$  and the completion at  $i = L$  [13]. Analysis of this distribution and showing its very simple limiting behavior is the main contribution of our work.

We note that, even though a lot is known about the first passage times in different scenarios [13, 14] and about temporal dynamics of KPR schemes [10, 11], to our knowledge, the first passage for KPR has not been analyzed rigorously.

We consider three different cases of the gKPR scheme depicted in Fig. 1, each corresponding to a different con-

tinuous time / discrete space Markov chain with exponential transition times (our results can be generalized to the case of non-exponential distribution of transition times using the methods of [15]). First is a normal random walk (RW) process (that is  $\gamma = 0$ ) with an absorbing boundary at  $i = L$  and a reflecting boundary at  $i = 0$ . This model is denoted as the transmission mode (TM) process [13]. The second model is the directed KPR (dKPR) scheme where ( $k > 0, r = 0, \gamma > 0$ ). Finally, the third model is the full gKPR process, where all rates are non-zero. For each model, we provide exact solutions for the escape time distributions in the Laplace domain and explicit expressions for the mean and variances of the escape times (see *Materials and Methods*). Further, we discuss how these distributions change as the system parameters are adjusted and expose regimes where the processes transition from one simple behavior to another.

## II. RESULTS

### A. Transmission Mode (TM)

For the TM process, in which the forward and backward rates ( $k$  and  $r$ ) are non-zero, one can derive explicit expressions for the mean and the variance of the first passage time (see *Materials and Methods: Transmission Mode*). Defining  $\theta = r/k$ , these can be written:

$$\mu_{\text{TM}} = \frac{1}{k} \frac{L - (L+1)\theta + \theta^{L+1}}{(1-\theta)^2}, \quad (1)$$

$$\sigma_{\text{TM}}^2 = \text{CV}_{\text{TM}}^2 \mu_{\text{TM}}^2, \quad (2)$$

$$\text{CV}_{\text{TM}}^2 = \frac{L - 4\theta - (L+1)\theta^2 + 4(L - L\theta + 1)\theta^{L+1} + \theta^{2L+2}}{(L - L\theta + \theta[\theta^L - 1])^2}, \quad (3)$$

where  $\text{CV}_{\text{TM}}$  is called the *coefficient of variation*. For a deterministic process,  $\text{CV} = 0$ , and for an exponentially distributed one,  $\text{CV} = 1$ . This makes the coefficient of variation a useful property characterizing a distribution.

Fig. 2A-C shows the effects that changes in the parameters  $\theta$  and  $L$  have on the distribution of the escape time. In order to show the distribution for diverse parameters simultaneously, time has been rescaled by the mean  $\mu$  for each curve,  $\tau = t/\mu$ . This leads to the probability density  $f(\tau) = \mu f(t)$ . Fig. 2A shows that, for a fixed  $L$ , as  $\theta$  increases, the distribution becomes broader and approaches an exponential distribution, while as  $\theta$  decreases the distribution approaches a  $\Gamma$ -distribution,  $\Gamma(L, 1/k)$ . In order to quantify these behaviors we provide the trends of the mean and the coefficient of variation for the cor-

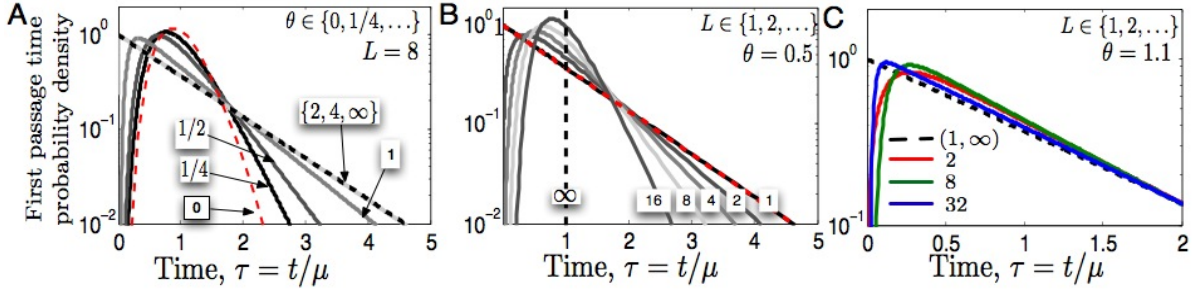


FIG. 2: Effect of changing  $\theta = r/k$  and  $L$  on the first passage time distribution for the TM process. The time been rescaled for each curve as  $\tau = t/\mu$ . (A) First passage time distribution for different values of the backward rate,  $r$ , and a fixed length  $L = 8$ . Here  $r$  ranges from  $k/4$  to  $4k$ , as denoted in the boxes. The two dashed lines correspond to the limiting cases,  $\theta = 0, \infty$  ( $\Gamma$ -distribution and an exponential, respectively). (B,C) Effect of changing the length  $L$  on the escape time distribution (B) for  $\theta = 0.5$  and (C) for  $\theta = 1.1$ . For  $\theta < 1$ , the limiting behavior as  $L \rightarrow \infty$  is a delta function; for  $\theta > 1$ , the limiting distribution is the exponential.

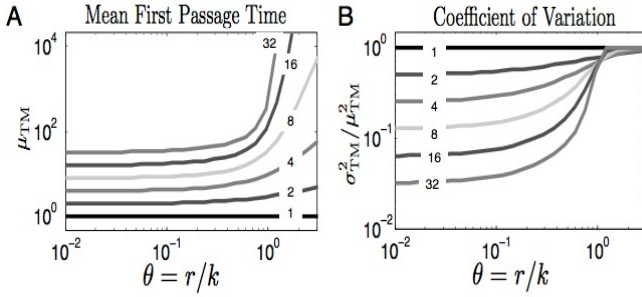


FIG. 3: Effect of changing the length or backward rate,  $r$ , on the mean (A) and squared coefficient of variation (B) of the TM process first passage times. The curves have been computed using Eqns. (1, 3) and are plotted for increasing values of  $L = \{1, 2, 4, 8, 16, 32\}$ .

responding regimes.

$$\mu_{\text{TM}}(L, \theta) \approx \begin{cases} \theta^{L-1}/k & \text{for } \theta \gg 2, \\ L/k & \text{for } \theta \ll \frac{L}{L-1}, \end{cases} \quad (4)$$

$$\text{CV}_{\text{TM}}^2(L, \theta) \approx \begin{cases} 1 - 2(L-1)/\theta^L & \text{for } \theta \gg \frac{L+2}{L-1}, \\ 1/L & \text{for } \theta \ll \frac{L}{2(L-1)}. \end{cases} \quad (5)$$

It is worth mentioning that  $\theta = 1$  means an unbiased random walk, while  $\theta < 1 (> 1)$  means a walk biased towards the entry (exit) point.

Figs. 2B, C show that changes in  $L$  have different effects on the escape time distribution depending upon the value of  $\theta$ . When  $\theta < 1$ , the limiting distribution as  $L$  becomes large is a  $\delta$ -function at  $t = L/[k(1-\theta)]$ , whereas for  $\theta > 1$ , the limiting distribution is an exponential with  $\mu_{\text{TM}} = \theta^{L+1}/[k(1-\theta)^2]$ .

Fig. 3 illustrates the effect that changes in  $L$  and  $\theta$  have on  $\mu_{\text{TM}}$  and  $\text{CV}_{\text{TM}}^2$ , as given by Eqns. (1, 3). It is of particular interest to examine these as the chain becomes long. From Eq. (3), we see that, as  $L$  increases,

$\text{CV}_{\text{TM}}^2$  converges point-wise to the step function:

$$\lim_{L \rightarrow \infty} \text{CV}_{\text{TM}}^2(L, \theta) = u(\theta - 1) = \begin{cases} 0 & \text{for } \theta < 1, \\ 1 & \text{for } \theta > 1. \end{cases} \quad (6)$$

Numerical analysis of Eq. 3 around  $\theta = 1$ , shows that the maximum slope of  $\text{CV}_{\text{TM}}^2$  (to leading order in  $L$ ) occurs at a point that approaches  $\theta = 1$  at a rate:

$$1 - \arg \max_{\theta} \frac{d\text{CV}_{\text{TM}}^2}{d\theta} = \frac{21}{2L^2} + \mathcal{O}(L^{-3}). \quad (7)$$

The slope at  $\theta = 1 - 21/(2L^2)$  is:

$$\max_{\theta} \frac{d\text{CV}_{\text{TM}}^2}{d\theta} = \frac{4}{45}L + \mathcal{O}(1). \quad (8)$$

Thus for a given large  $L$ , the range of  $\theta$  over which the first passage time changes from a narrow  $\Gamma$ -distribution to a broad exponential distribution is centered just left of  $\theta = 1$ , and it becomes increasingly narrow as  $L$  increases.

## B. Directed Kinetic Proofreading (dKPR)

For the dKPR process, the system can return directly to the origin with rate  $\gamma > 0$ , but the backward rate,  $r$ , is zero. Then, defining  $\psi = \gamma/k$ , the mean and the coefficient of variation of the first passage times are (see *Materials and Methods: Directed Kinetic Proofreading*):

$$\mu_{\text{dKPR}} = \frac{1}{k\psi} \left[ (1 + \psi)^L - 1 \right], \quad (9)$$

$$\text{CV}_{\text{dKPR}}^2 = \frac{(1 + \psi)^{2L} - 2\psi L (1 + \psi)^{L-1} - 1}{(1 + \psi)^{2L} - 2(1 + \psi)^L + 1}, \quad (10)$$

Fig. 4A-B shows the effects that changes in  $\psi$  and  $L$  have on the distribution of the waiting times for the dKPR process. As in the previous section, time has been rescaled by  $\mu$  for each curve. For a fixed  $L$ , as  $\psi$  increases, the distribution again approaches either an exponential

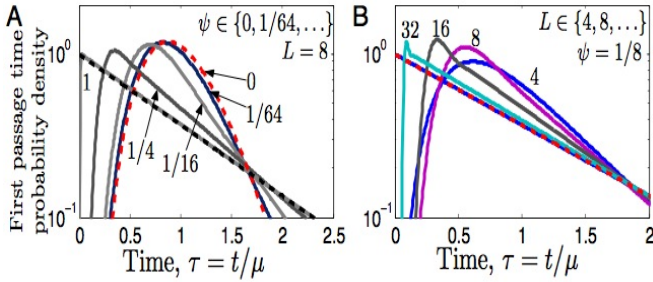


FIG. 4: Effect of changing  $\psi = \gamma/k$  and  $L$  on the first passage time distribution (normalized by its mean) for the dKPR process. (A) The first passage time distribution for different values of the return rate,  $\gamma$  and a fixed length  $L = 8$ . The parameter  $\psi$  ranges from  $1/64$  to  $1$  as denoted in the figure. The two dashed lines correspond to the limiting cases, where  $\psi = 0, \infty$ . The former results in a  $\Gamma$ -distribution, and the latter in an exponential distribution. (B) Effect of changing the length  $L$  on the first passage time distribution for  $\psi = 1/8$ . For any value of  $\psi > 0$ , the limiting behavior as  $L \rightarrow \infty$  is an exponential distribution.

distribution or  $\Gamma$ -distribution for  $\gamma \rightarrow \infty, 0$ , respectively. Unlike for the TM process, the limiting distribution as  $L \rightarrow \infty$  is exponential for any value of  $\psi > 0$ .

In Fig. 5, we illustrate the dependence of  $\mu_{\text{dKPR}}$  and  $\text{CV}_{\text{dKPR}}^2$  on  $L$  and  $\psi$ . From Eqns. (9, 10), their limiting behaviors are:

$$\mu_{\text{dKPR}}(L, \psi) \approx \begin{cases} \psi^{L-1}/k & \text{for } \psi \gg L, \\ L/k & \text{for } \psi \ll L/2, \end{cases} \quad (11)$$

$$\text{CV}_{\text{dKPR}}^2(L, \psi) \approx \begin{cases} 1 - 2(L-1)/\psi^L & \text{for } \psi \gg 2L, \\ 1/L & \text{for } \psi \ll 3/L^2. \end{cases} \quad (12)$$

Furthermore, as  $L$  grows, the coefficient of variation tends to converge point-wise to a step function at  $\psi = 0$ :

$$\lim_{L \rightarrow \infty} \text{CV}_{\text{dKPR}}^2 = \begin{cases} 0 & \text{for } \psi = 0, \\ 1 & \text{for } \psi > 0. \end{cases} \quad (13)$$

As in the TM process, this convergence can be studied by examining the maximum slope of the coefficient of variation. Since the second derivative of  $\text{CV}_{\text{dKPR}}^2$  is always negative for  $\psi \geq 0$ , this maximum slope occurs at  $\psi = 0$ . Taking the derivative of Eqn. 10 at the point  $\psi = 0$  yields an exact expression for the maximal slope,

$$\max_{\psi} \frac{d\text{CV}_{\text{dKPR}}^2}{d\psi} = \left. \frac{d\text{CV}_{\text{dKPR}}^2}{d\psi} \right|_{\psi=0} = \frac{L^2 - 1}{3L}. \quad (14)$$

These trends are readily apparent in Fig. 5B, where as  $L$  or  $\psi$  increase,  $\text{CV}^2$  approaches unity.

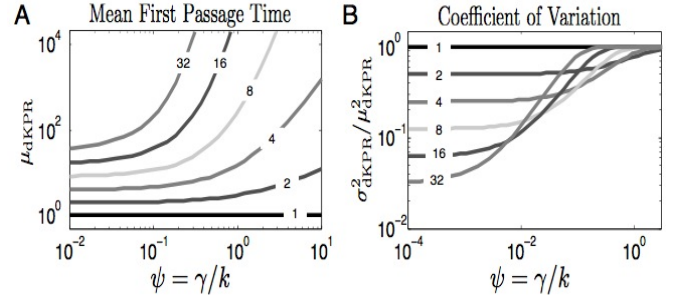


FIG. 5: Effect of changing the length or the proofreading rate,  $\gamma$ , on the mean (A) and the squared coefficient of variation (B) of the escape time for the dKPR system. The curves have been computed analytically using Eqns. (9, 10) and are plotted for increasing values of  $L = \{1, 2, 4, 8, 16, 32\}$ .

### C. Comparison between the TM and the dKPR models

The TM and the dKPR processes exhibit very similar behaviors in their first passage time distributions: for a fixed large  $L$ , increases in  $\theta$  or  $\psi$  result in sharp transitions from deterministic to exponential completion times. Moreover, the two processes have *quantitatively* the same limiting behaviors on either side of the transition: the means and the CVs are asymptotically the same functions of  $\theta$  and  $\psi$  [cf. Eqns. (4, 5, 11, 12)].

However, the similarity between the limits of both processes is not exact. For the TM, the deterministic-to-exponential transition (defined by the point of the maximum slope of  $\text{CV}^2$ ) is near  $\theta = 1$ , approaching it as  $L$  grows [cf. Eq. (7)], while the same transition for the dKPR is always at  $\psi = 0$ . Moreover, although for both models the width of the transition region, as defined by the maximum slope of  $\text{CV}^2$ , is inversely proportional to the system size (for  $L \gg 1$ ), the width is  $15/4$  times larger for the TM process. Finally, while the small/large  $\theta$  and  $\psi$  limits are the same in both models, the terms *small* and *large* themselves have different meanings. In particular, for the TM model the meanings are effectively independent of the system size (Eqn. (5)), while for the dKPR model the meanings strongly depend on  $L$  (Eqn. (12)).

### D. General Kinetic Proofreading (gKPR)

In the most general case, both  $r > 0$ , and  $\gamma > 0$ . Still, one can derive explicit expressions for the mean and variance of the first passage times [see Eqns. (38, 39) in *Materials and Methods*]. Fig. 6 illustrates the probability distribution for the exit times of the gKPR process for different  $\theta$ ,  $\psi$ , and  $L$ . Based upon the previous results, it is no surprise that the escape time distributions converge to an exponential distribution as  $\psi$  or  $\theta$  are large (cf. Fig. 6A, B), or to a  $\Gamma$ -distribution when  $\psi = \theta = 0$ . It is also not surprising that the gKPR first passage time distribu-

tion converges to an exponential distribution when  $\gamma > 0$  and  $L$  is large (cf. Fig. 6C). What is surprising is how neatly the two constituent processes, TM and dKPR, combine to define the trends of the gKPR process. Figs. 7A-D show the mean and the coefficient of variation of the first passage time distributions for this process under various conditions. In panel A, we plot  $\mu_{\text{gKPR}}$  as a function of  $\theta$  and  $\psi$  for a fixed system size of  $L = 8$ , and panel B shows the corresponding  $\text{CV}_{\text{gKPR}}^2$ . Panels C and D show the same information, but for  $L = 16$ . We see that the general trend for the increase in the mean passage time and the convergence of the  $\text{CV}^2$  are determined in the same manner as those for the TM and dKPR processes. In particular, we find that the contour lines for both  $\mu_{\text{gKPR}}$  and  $\text{CV}_{\text{gKPR}}^2$  are almost linear. However, this linearity is not exact—the actual contour lines for  $\mu_{\text{gKPR}}(\psi, \theta)$  are slightly concave and the contour lines for  $\text{CV}_{\text{gKPR}}^2(\psi, \theta)$  are slightly convex. From Figs. 3 and 5 above, we see that changes in  $L$  have a large effect on the first passage time of the TM and dKPR processes particularly around  $\theta = 1$  and  $\psi = 0$ , respectively. In the gKPR process, these effects correspond to changes in the endpoints, and therefore the slopes of the contour lines in Fig. 7A-D.

With explicit expressions for the mean and coefficient of variation, one can again examine their limiting behaviors for growing  $\psi$  and  $\theta$ . In particular, we find that these are equal to those of the TM and the dKPR models when  $\theta \rightarrow \infty$  or  $\psi \rightarrow \infty$ , respectively. Further, if  $L$  is large and  $\psi > 0$ , the mean first passage is:

$$\lim_{L \rightarrow \infty} \mu_{\text{gKPR}} \approx \frac{(l_+ \theta)^L}{2k\psi} \left( 1 + \frac{1 - \theta + \psi}{\sqrt{(1 + \theta + \psi)^2 - 4\theta}} \right), \quad (15)$$

where

$$l_+ \theta = \frac{1 + \theta + \psi + \sqrt{(1 + \theta + \psi)^2 - 4\theta}}{2} \geq 1. \quad (16)$$

Further, the coefficient of variation,  $\text{CV}_{\text{gKPR}}^2$  approaches unity for all values except when  $\psi = 0$  and  $\theta < 1$ , and

$$\text{CV}_{\text{gKPR}}^2(L, \theta) \approx \begin{cases} 1 - \frac{2(L-1)}{(\psi+\theta)^L} & \text{for } \psi \gg 2L \text{ and } \theta \gg 4, \\ 1/L & \text{for } \psi \ll \frac{L^2}{3} \text{ and } \theta \ll \frac{1}{2}. \end{cases} \quad (17)$$

This shows that, for large proofreading and backward rates, the two effects have equal influences on the distribution of the completion time. However, one should bear in mind that, again, the meaning of small/large  $\theta, \psi$  is different.

### III. DISCUSSION

The results for the coefficient of variation of the escape time distribution, as well as the shapes of the distributions themselves, clearly show that the KPR process has two simple limiting behaviors as the system size

increases. First, when the overall bias is forward, the completion time becomes narrowly distributed. Second, when the overall bias is backward, the escape time distribution approaches an exponential. Both of these behaviors are substantially simpler than one could have expected from the original complex kinetic diagram, implying that the observable behavior of this complex system can be approximated accurately by a single-parameter equivalent, corresponding either to a deterministic reaction or a simple two-state Markov chain. Interestingly, the approach to the deterministic regime as the system size grows is well understood (see, for example, [16] on the discussion of this effect in the context of reproducibility of responses of rod cells to single photon capture events). However, the exponential regime has not been explored extensively before, even though it is the more robust of the two, emerging for any  $\psi > 0$ .

Both limiting behaviors of the KPR system are explainable by simple intuitive arguments. First, a system with a forward bias completes the entire process in a certain characteristic time, and the relative standard deviation of this time scales as  $1/\sqrt{\text{number of steps}}$ , as is always the case for the addition of independent identically distributed random variables. In the opposite case, the backward bias ensures that the process repeatedly returns to the initial state, from which many *independent* escape attempts are made. Due to the independence, the number of such attempts before a success has a geometric distribution (the discrete analog of an exponential distribution), and its form effectively defines the first passage time distribution. In other words, the system tries to climb out of a free energy well (with the ground state near the entry point), and escape times in such cases are usually exponentially distributed.

Although the KPR model described here is a relatively simple linear chain processes with site-independent transition rates, the conclusions we make generalize to more complicated systems. First, when the rates  $k, r, \gamma$  are site-specific, time scale separations and averaging techniques will allow for the reduction to simpler processes comprising a more narrowly distributed set of parameters. Second, if biochemical processes involve multiple independent pathways, each with exponential/deterministic waiting times, then the first of these pathways to complete will also be exponential/deterministic. Similarly, first passage times for higher dimensional random walks also frequently exhibit simplified dynamics, as has been shown via reductions to a stochastic model of the genetic toggle switch [17]. Finally, the “well” argument says that the overall bias of a system’s motion will control the choice between the exponential (Markovian) and the deterministic behaviors even for more complex systems. In particular, it is clear that any KPR-like system, where a strong backward bias helps to undo potential mistakes, is likely to fall in the exponential escape time distribution regime.

Given that so much structural complexity is used to achieve a very simple dynamics in these processes, it is

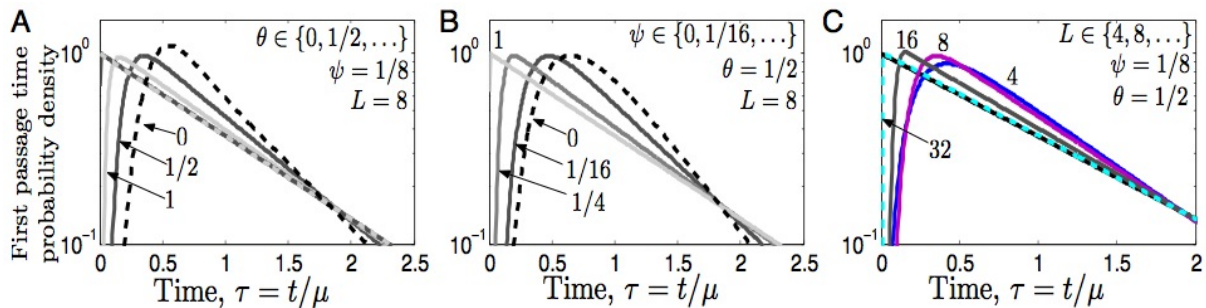


FIG. 6: The escape time probability density function for the gKPR scheme. (A)  $\psi = \gamma/k = 1/8$ ,  $L = 8$ , and variable of  $\theta = r/k$ . (B)  $\theta = 1/2$ ,  $L = 8$  and variable  $\psi$ . (C)  $\theta = 1/2$ ,  $\psi = 1/8$ , and variable  $L$ . In all cases, the limiting behavior is an exponential as  $L$ ,  $\theta$ , or  $\psi$  grow.

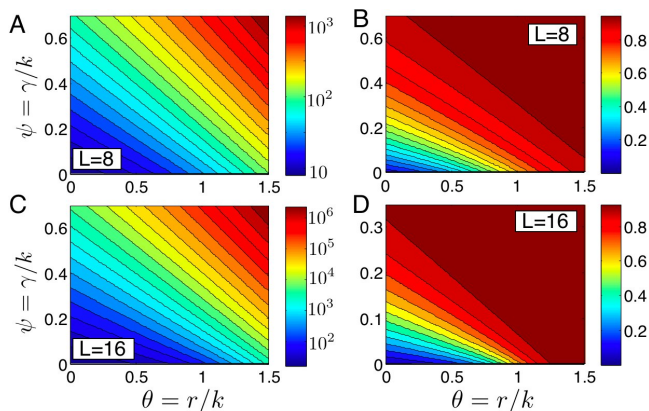


FIG. 7: Effects of parameter variation on the escape time distribution for the gKPR process. (A) Mean first passage time versus  $\theta$  and  $\psi$  for  $L = 8$ . (B) Coefficient of variation,  $CV_{\text{gKPR}}^2$  versus  $\theta$  and  $\psi$  for  $L = 8$ . (C, D) the same for  $L = 16$ .

natural to ask why the complexity is used at all. One hypothesis is that such agglomeration of multiple independent kinetic parameters into a few coarse-grained variables means that multiple chemotypes can result in the same phenotype. Thus, the system possesses *many* situationally *sensitive* knobs with which it can compensate for environmental changes and maintain *a few* simple behaviors. Such adaptive flexibility has been observed in a variety of contexts [20, 21, 22]. An alternative hypothesis may be that these extra elements are vestigial network components to which the cell is *insensitive* in its current evolutionary or developmental situation. The current work provides a starting point to evaluate these possibilities via parametric sensitivity analysis.

Finally, the fact that the KPR process, as well as many others, has such simple limiting behaviors has important consequences for the modeling of biochemical systems. The bad news is that it is unreasonable to hope to characterize individual molecular reactions with observations of the input-to-output responses—many different internal organizations will result in equivalent observable be-

haviors. The good news is that, when attempting to understand such processes in a wider cellular context, it is often unnecessary to explicitly treat every individual step—a coarse-grained model with only a handful of aggregate parameters may be sufficient. This result clearly explains why simple phenomenological Markovian reaction rate models of complicated processes, such as transcription, translation, enzyme activation and others, have had such a great success in explaining biological data.

## IV. MATERIALS AND METHODS

### A. Preliminaries

Let the vector  $\mathbf{p} = [p_0(t), p_1(t), \dots, p_L(t)]^T$  denote the probabilities of each state in the kinetic diagram in Fig. 1. This distribution evolves according to the Master Equation (ME), which can be written:  $\dot{\mathbf{p}}(t) = \mathbf{A}\mathbf{p}(t)$ , where the infinitesimal generator matrix  $\mathbf{A}$  is:

$$A_{ij} = \begin{cases} -k & \text{for } i = j = 0, \\ -k - \gamma - r & \text{for } 0 < i = j \leq L - 1, \\ \gamma + r & \text{for } (i, j) = (0, 1), \\ \gamma & \text{for } i = 0 \text{ and } 2 \leq j \leq L - 1, \\ r & \text{for } i = j - 1 \text{ and } 2 \leq j \leq L - 1, \\ k & \text{for } i = j + 1 \text{ and } 2 \leq j \leq L - 1, \\ 0 & \text{everywhere else.} \end{cases} \quad (18)$$

By applying the Laplace transform,

$$P_i(s) = \int_0^\infty p_i(t) e^{-st} dt, \quad (19)$$

one can convert the ME to a set of linear algebraic equations:

$$(s - \mathbf{A}) \mathbf{P}(s) = \mathbf{p}(t = 0) \equiv \mathbf{e}_0. \quad (20)$$

Note that this equation includes the specification of the initial condition,  $p_i(t = 0) = \delta_{i,0}$ , where  $\delta$  is the Kronecker delta.

We now construct a general solution for this equation in the form

$$P_i(s) = C_1 \lambda_1^i + C_2 \lambda_2^i. \quad (21)$$

Inserting this into the expression for  $0 < i < L - 1$ , one finds that the space-independent parameters  $\lambda_{1,2}$  satisfy

$$\frac{k}{s+k+\gamma+r} + \frac{r}{s+k+\gamma+r} \lambda^2 - \lambda = 0. \quad (22)$$

Similarly, the coefficients  $C_1$  and  $C_2$  must obey the equations for  $P_0(s)$  and  $P_{L-1}(s)$  in (20), which can be written as

$$(s+k)(C_1+C_2) = 1 + r(C_1\lambda_1 + C_2\lambda_2) + \gamma \left( C_1 \left[ \frac{1-\lambda_1^L}{1-\lambda_1} - 1 \right] + C_2 \left[ \frac{1-\lambda_2^L}{1-\lambda_2} - 1 \right] \right) \quad (23)$$

$$C_1\lambda_1^{L-1} + C_2\lambda_2^{L-1} = \frac{k}{s+k+r+\gamma} (C_1\lambda_1^{L-2} + C_2\lambda_2^{L-2}), \quad (24)$$

where we have applied the geometric series identity,  $\sum_{i=1}^{L-1} \lambda^i = \frac{1-\lambda^L}{1-\lambda} - 1$ .

Since  $P_L(t)$  is the cumulative probability that the system has reached the absorbing state, the first passage time probability density,  $f(t) = dp_L(t)/dt$ , can be written in the Laplace domain as:

$$F(s) = kP_{L-1}(s). \quad (25)$$

Once this quantity is known, all uncentered moments of the escape time are easily derived as

$$T^{(m)} = \int_0^\infty t^m f(t) dt = (-1)^m \left. \frac{dF(s)}{ds} \right|_{s=0}. \quad (26)$$

With this in mind, we now consider the three special cases in the following subsections.

### B. Transmission Mode

The first case to be considered is transmission mode: the continuous time, discrete space random walk, where the process can only move forward or backward to its nearest neighbor. Applying the boundary conditions as expressed in Eq. (24) yields the expressions for  $C_1$  and  $C_2$ :

$$C_1 = \frac{1}{(s+k-r\lambda_2) \left[ \frac{\lambda_2-1}{\lambda_1-1} - \left( \frac{\lambda_1}{\lambda_2} \right)^L \right]}, \text{ and } C_2 = -C_1 \frac{\lambda_1^L}{\lambda_2^L}, \quad (27)$$

where  $\lambda_1$  and  $\lambda_2$  are obtained from Eq. (22):

$$\lambda_{1,2} = \frac{s+k+r \pm \sqrt{(s+k+r)^2 - 4kr}}{2r}. \quad (28)$$

Following simple algebra, the Laplace transform of the first passage time probability density function (PDF) then becomes

$$F(s) = C_1 k \lambda_1^{L-1} \left( 1 - \frac{\lambda_1}{\lambda_2} \right), \quad (29)$$

from which all moments of the first passage time can be extracted. In particular the mean escape time and the variance are given by Eqs. (1, 2) in the main text.

### C. Directed Kinetic Proofreading

The second case we consider is that of directed kinetic proofreading, in which the backward transition rate is neglected,  $r = 0$ , but the return rate is non-zero,  $\gamma > 0$ . In this case the solution is much simpler and can be written as

$$\tilde{p}_i(s) = C_1 \lambda^i, \quad (30)$$

where  $\lambda$  is the single root of Eq. (22) given by

$$\lambda = \frac{k}{s+k+\gamma}, \quad (31)$$

and the coefficient  $C_1$  is reduced to

$$C_1 = \frac{1}{s+k-\gamma \left( \frac{1-\lambda^L}{1-\lambda} - 1 \right)}. \quad (32)$$

In this case, the Laplace transform of the first passage time is given by

$$f(s) = k p_{L-1}(s) = \frac{k}{s+k-\gamma \left( \frac{1-\lambda^L}{1-\lambda} - 1 \right)} \lambda^{L-1}, \quad (33)$$

which gives the expressions for the mean escape time and its coefficient of variation as in Eqs. (9, 10) in the main text.

### D. General Kinetic Proofreading

In this case, all the rates  $k$ ,  $\gamma$ , and  $r$  are non-zero, and Eq. (22) has two solutions

$$\lambda_{1,2} = \frac{s+k+r+\gamma \pm \sqrt{(s+k+r+\gamma)^2 - 4kr}}{2r}. \quad (34)$$

By applying the boundary conditions in Eq. (24), we obtain the expressions for  $C_1$  and  $C_2$ :

$$C_1 = \frac{1}{r(\lambda_2-1) - \gamma \frac{1-\lambda_1^L}{1-\lambda_1} + \left( \frac{\lambda_1}{\lambda_2} \right)^L \left( r(1-\lambda_1) + \gamma \frac{1-\lambda_2^L}{1-\lambda_2} \right)} \quad (35)$$

$$C_2 = -C_1 \left( \frac{\lambda_1}{\lambda_2} \right)^L, \quad (36)$$

with which one can define the Laplace transform of the first passage time PDF:

$$F(s) = C_1 k \lambda_1^{L-1} \left( 1 - \frac{\lambda_1}{\lambda_2} \right). \quad (37)$$

Once again, it is possible to derive the the mean and variance of the escape time in this scheme

$$\mu_{\text{gKPR}} = \frac{1}{2k\psi} \left[ \frac{1-\theta+\psi}{\sqrt{(1+\theta+\psi)^2 - 4\theta}} \left( l_+^L - l_-^L \right) \theta^L + \left( l_+^L + l_-^L \right) \theta^L - 2 \right], \quad (38)$$

where  $l_{\pm}$  are defined as in Eq. (16). The first passage time variance in this case is given by

$$\begin{aligned}
k^2 \psi^2 \sigma_{\text{gKPR}}^2 &= \frac{1}{2} \theta^{2L} \left( l_{-}^{2L} + l_{+}^{2L} \right) - 1 \\
&+ \frac{\theta^{2L-1} (\theta - 1 - \psi) (l_{-}^{2L} - l_{+}^{2L}) + 2L\psi\theta^{L-1} (l_{-}^L - l_{+}^L)}{2(l_{+} - l_{-})} \\
&+ \psi \frac{2\theta - L (l_{-}^L + l_{+}^L) (-\theta + 1 + \psi) \theta^{L-2} - \theta^{2L-1} (l_{-}^{2L} + l_{+}^{2L})}{(l_{+} - l_{-})^2} \\
&- \frac{2\psi (1 - \theta^{L-1})}{(l_{+} - l_{-})^2} + \frac{2\theta^{L-2} \psi (\theta - 1 + \psi) (l_{-}^L - l_{+}^L)}{(l_{+} - l_{-})^3}. \quad (39)
\end{aligned}$$

## Acknowledgments

We thank N. Sinitzyn for engaging discussion during early stages of this work. We also thank B. Goldstein, R. Gutenkunst, and M. Monine. This work was funded by LANL LDRD program under DOE Contract No. DE-AC52-06NA25396.

- 
- [1] Faeder, J et al. (2003) Investigation of early events in FceRI-mediated signaling using a detailed mathematical model. *J. Immunol.* 170:3769–3781.
- [2] Hopfield, J (1974) Kinetic proofreading: A new mechanism for reducing errors in biosynthetic processes requiring high specificity. *Proc. Natl. Acad. Sci. (USA)* 71:4135–4139.
- [3] Yan, J, Magnasco, M, Marko, J (1999) A kinetic proofreading mechanism for disentanglement of DNA by topoisomerases. *Nature* 401:932–935.
- [4] Sancar, A, amd K. Unsal-Kacmaz, LLB, Linn, S (2004) Molecular mechanisms of mammalian DNA repair and the DNA damage checkpoints. *Annual Rev. Biochem.* 73:39–85.
- [5] Blanchard, S, R. G., J, Kim, H, Chu, S, Puglist, J (2004) tRNA selection and kinetic proofreading in translation. *Nature Struct. Mol. Biol.* 11:1008–1014.
- [6] Jovanovic-Talisman, T et al. (2008) Artificial nanopores that mimic the transport selectivity of the nuclear pore complex. *Nature* 457:1023.
- [7] McKeithan, T (1995) Kinetic proofreading in T-cell receptor signal transduction. *Proc. Natl. Acad. Sci. (USA)* 92:5042–5046.
- [8] Rabinowitz, J, Beeson, C, Lyons, D, Davis, M, McConnell, H (1996) Kinetic discrimination in T-cell activation. *Proc. Natl. Acad. Sci. (USA)* 93:1401–1405.
- [9] Rosette, C et al. (2001) The impact of duration versus extent of tcr occupancy of t cell activation: A revision of the kinetic proofreading model. *Immunity* 15:59–70.
- [10] Liu, Z, Haleem-Smith, H, Chen, H, Metzger, H (2001) Unexpected signals in a system subject to kinetic proofreading. *Proc. Natl. Acad. Sci. (USA)* 98:7289–7294.
- [11] Goldstein, B, Faeder, J, Hlavacek, W (2004) Mathematical and computational models of immune-receptor signalling. *Nature Rev. Immunol.* 4:445–456.
- [12] Hlavacek, W, Redondo, A, Wofsy, C, Goldstein, B (2002) Kinetic proofreading in receptor-mediated transduction of cellular signals: Receptor aggregation, partially activated receptors, and cytosolic messengers. *Bull. Math. Biol.* 64:887–911.
- [13] Redner, S (2001) *A Guide To First-Passage Processes* (Cambridge University Press).
- [14] Dorsogna, M, Chou, T, (2005) First Passage and Cooperativity of Queuing Kinetics *Phys. Rev. Lett.* 95:170603.
- [15] Bel, G, Barkai, E (2006) Random walk to a nonergodic equilibrium concept. *Phys. Rev. E* 73:016125.
- [16] Doan, T, Mendez, A, Detwiler, P, Chen, J, Rieke, F (2006) Multiple phosphorylation sites confer reproducibility of the rod’s single-photon responses. *Science* 313:530.
- [17] Munsky, B, Khammash, M (2008) Transient Analysis of Stochastic Switches and Trajectories with Applications to Gene Regulatory Networks *IET Systems Biology* 2:323-333.
- [18] Gardner, T, Cantor, C, Collins, J (2000) Construction of a genetic toggle switch in *Escherichia coli* *Nature* 403:339-24.
- [19] Swain, P, Elowitz, M, Siggia, E (2002) Intrinsic and extrinsic contributions to stochasticity in gene expression. *Proc. Natl. Acad. Sci. (USA)* 9:12795.
- [20] Stern, S, Dror, T, Stolovicki, E, Brenner, N, Braun, E (2007) Genome-wide transcriptional plasticity underlies cellular adaptation to novel challenge. *Mol. Syst. Biol.* p 106.
- [21] Ziv, E, Nemenman, I, Wiggins, C (2007) Optimal information processing in small stochastic biochemical networks. *PLoS ONE* 2:e1077.
- [22] Gutenkunst, R et al. (2007) Universally sloppy parameter sensitivities in systems biology. *PLoS Comput. Biol.* 3:e189.